

## Short-range order and its effect on the electronic structure of binary alloys: CuZn – a case study

ABHIJIT MOOKERJEE<sup>1,4,\*</sup>, KARTICK TARAFDER<sup>2</sup>,  
ATISDIPANKAR CHAKRABARTI<sup>2,5</sup> and KAMAL KRISHNA SAHA<sup>3</sup>

<sup>1</sup>Department of Physics, Indian Institute of Technology, Kanpur 208 016, India

<sup>2</sup>S.N. Bose National Center for Basic Sciences, JD Block, Sector III, Salt Lake City, Kolkata 700 098, India

<sup>3</sup>Theory Department, Max-Planck-Institut für Mikrostrukturphysik, Weinberg 2, D-06120 Halle (Saale), Germany

<sup>4</sup>On sabbatical leave from: S.N. Bose National Center for Basic Sciences, JD Block, Sector III, Salt Lake City, Kolkata 700 098, India

<sup>5</sup>Permanent address: Ramakrishna Mission Vivekananda Centenary College, Rahara, West Bengal, India

\*Corresponding author. E-mail: abhijit@bose.res.in

**Abstract.** We discuss an application of the generalized augmented space method introduced by one of us combined with the recursion method of Haydock *et al* (GASR) to the study of electronic structure and optical properties of random binary alloys. As an example, we have taken the 50-50 CuZn alloy, where neutron scattering indicates the existence of short-range order.

**Keywords.** Disordered alloys; short-range order; optical conductivity.

**PACS Nos** 61.46.+w; 36.40.Cg; 75.50.Pp

### 1. Introduction

The first-principles theoretical study of the electronic structure of disordered alloys has had a distinguished history since the early 1960s. Of the many first-principles electronic structure methods for disordered alloys in vogue these days, we shall identify a few which we believe to be the most accurate. We shall try to provide insights into the advantages and drawbacks of these techniques and provide confidence in their use for future studies on different alloy systems.

We have identified three electronic structure methods for disordered substitutional binary alloys: the Korringa–Kohn–Rostocker-based mean field coherent potential approximation (KKR-CPA) [1], the KKR-based super-cell calculations on special quasi-random structures (KKR-SQS) [2] and the tight-binding linear muffin-tin orbitals based augmented space recursion (TB-LMTO-ASR) [3]. The KKR and its linear version, LMTO, are among the accurate techniques in use for the study

of random substitutional alloys, where the disorder-induced scattering is local. Of course, LMTO being a linearized approximation to the KKR, is expected to be less accurate. However, if the energy window around the linearization energy nodes is not too large, the LMTO estimates energies with tolerances of around 50–100 mRyd. Unless we are interested in estimating energy differences smaller than this quantity or over large energy windows, the LMTO is good enough and has the great advantage that its secular equation is an eigenvalue problem rather than the more complicated functional equation of the KKR. We shall use all three of these methods and compare and contrast the corresponding results.

Methods to deal with disorder fall into three categories. First is the single-site mean-field CPA. This approximation has been eminently successful in dealing with a variety of disordered systems. However, whenever there is either strong disorder fluctuation scattering, as in dilute, split-band alloys or when local environment effects like short-ranged ordering, clustering and segregation, or local lattice distortions due to size mismatch of the constituent atoms become important, the single-site based CPA becomes inadequate.

In the second category belong the generalizations of the CPA, of which, the augmented space-based methods such as the itinerant CPA [4] (ICPA) and the augmented space recursion (ASR) [5,6], are foremost. They not only retain the necessary analytic (Herglotz) properties of the averaged Green function, as the CPA does, but also properly incorporate local environment effects.

In the third category belong the super-cell-based calculations. Zunger *et al* [2] suggested that if we construct a super-cell and populate its lattice points randomly by the constituents so as to mimic the concentration correlations in the random alloy, a single calculation with this super-lattice should approximate the configuration average in the infinite random system. This special quasi-random structure (SQS) approach has been used to incorporate short-ranged order and local lattice distortions in alloy systems [2]. Certainly, in the limit of a very large super-cell this statement is the theorem of spatial ergodicity. This theorem provides the explanation of why a single experiment on global property of a bulk material most often produces the configuration averaged result, provided the property we are looking at is self-averaging. How far this approach is accurate with a small cluster of, say, 16 atoms, is *a priori* uncertain.

Before we go on to describe the TB-LMTO-ASR and its generalization to deal with short-range order, let us examine the specific alloy system of interest to us in this area: namely, 50-50 CuZn. These alloys have a stable low-temperature  $\beta$ -phase which sits immediately to the right of the pure face-centered cubic Cu phase in the alloy phase diagram [7,8]. This phase, called  $\beta$ -brass, has a body-centered cubic structure. At high temperatures the alloy forms a disordered body-centered cubic structure. At around 730 K it orders into the B2 structure with two atoms per unit cell. The alloy satisfies the Hume-Rothery rules [9] and has the same ratio of valence electrons to atoms. Jona and Marcus [7] have shown from a density functional theory (DFT) based approach that within the local density approximation (LDA), it is the body-centered based B2 which is the stable ground state. They also showed that if we include the gradient corrections (GGA) then we get a tetragonal ground state lower in energy by 0.1 mRy/atom. This is in contradiction with the latest experimental data. The alloying of face-centered cubic Cu with an equal amount of

Zn leads to a body-centered stable phase. Zn has only one electron more than Cu. This is an interesting phenomenon. CuZn alloys also have anomalously high elastic anisotropy. This makes the theoretical study of CuZn an interesting exercise for a proposed theoretical technique.

One of the earliest first-principles density functional-based study of the electronic properties of CuZn was by Bansil and Ehrenreich [10]. The authors had studied the complex bands of  $\alpha$ -phase of CuZn using the Korringa–Kohn–Rostocker (KKR) method coupled with the coherent potential approximation (CPA) to take care of disorder. They commented on the effects of charge transfer and lattice constants on the electronic structure. They found the electronic distribution of this alloy to be of a split band kind with the centers of the Cu and Zn  $d$ -bands well separated from each other. Their Zn  $d$ -bands showed hardly any dispersion and were shown only schematically in their figures. In a later work, Rowlands *et al* [11] generalized the CPA to a non-local version (NL-CPA) and studied the effects of short-range ordering in CuZn. Their technique was based on an idea of renormalization in reciprocal space suggested by Jarrell and Krishnamurthy [12].

Early neutron scattering experiments were carried out on  $\beta$ -brass by Walker and Keating [13]. The Warren-Cowley short-range order parameter, defined by  $\alpha(R) = 1 - P_{AB}(R)/x$ , where  $x$  was the concentration of A and  $P_{AB}(R)$  was the probability of finding an A atom at a distance of  $R$  from a B atom, was directly obtained from the diffuse scattering cross-section:

$$\frac{d\sigma}{d\Omega} = x(1-x)(b_A - b_B)^2 \sum_R \alpha(R) f(K) \exp(iK \cdot R),$$

where  $b_A, b_B$  were the scattering lengths of A and B atoms, and  $f(K) = \exp(-C|K|^2)$  was the attenuation factor arising from thermal vibrations and static strains. The experimental data for the short-range order parameter as a function of temperature are thus available to us. An Ising-like model using pair interactions was studied by Walker and Chipman [14] and the short-range order was theoretically obtained. However, the pair interactions were simply fitted to the experimental values of the transition temperature  $T_C$  and in that sense it was an empirical theory. The experimental estimate of the nearest neighbour Warren-Cowley parameter was found to be varying between  $-0.171$  and  $-0.182$  at around 750 K.

In a later work using the much more sophisticated locally self-consistent Green function (LSGF) approach based on the tight-binding linear muffin-tin orbital (TB-LMTO) technique, Abrikosov *et al* [15] studied CuZn alloys. The authors argued that earlier studies of the mixing enthalpies of CuZn using the standard coherent potential approximation approaches [16–20] showed significant discrepancies with experiment. The discrepancies were assumed to partly arise from the neglect of charge transfer effects and partly because of short-ranged ordering (SRO). The main thrust of this technique, which was based on an earlier idea of a locally self-consistent multiple scattering (LSMS) by Wang *et al* [21], was to go beyond the CPA and include the effects of the immediate environment of an atom in the solid. The LSMS gave an excellent theoretical estimate of the ordering energy in CuZn: 3.37 mRy/atom as compared to the experimental value of 3.5 mRy/atom. The LSGF approach correctly predicted ordering tendency in CuZn on lowering temperature and combining with a cluster variation-Connolly Williams (CVM-CW)

obtained a value of the nearest neighbour Warren-Cowley SRO parameter  $\alpha = -0.15$ . Subsequently, Bruno *et al* [22] proposed a modification of the CPA including the local field effects and showed that charge transfer effects can be taken into account as accurately as the O(N) methods just described. They applied their approach to the CuZn alloys.

One of the earlier works on the optical property of CuZn alloy was the determination of the temperature variation of optical reflectivity by Muldrew [23]. The author attempted to explain the colour of the disordered  $\beta$ -brass CuZn alloy via the internal photoelectric effect [24]. Although the experimental data also contained the contribution from plasma oscillations, the author claimed that the optical reflectivity helps to explain the band picture of the alloys as a function of the inter-atomic spacing. In order to explain the optical properties, Amar *et al* [25–27] studied the band structure of CuZn using the KKR method. However, they had used the virtual crystal approximation, replacing the random potential seen by the electrons by an averaged one. This is now known to be particularly inaccurate for split band alloys.

The above discussion was necessary to bring into focus the following points: in the study of alloys like CuZn it would be interesting to address the effects of charge transfer and short-range ordering. In this communication we shall address exactly these two points. We shall propose the use of the augmented space recursion (ASR) coupled with the tight-binding linear muffin-tin orbitals basis (TB-LMTO) [5] to study the effects of short-range ordering on both the electronic structure and the optical properties of  $\beta$ -CuZn alloy at 50-50 composition. We would like to stress here that the TB-LMTO-ASR addresses precisely these effects with accuracy: the density functional self-consistent TB-LMTO takes care of the charge transfer, while the local environmental effects which are essential for the description of SRO are dealt with by the ASR. The TB-LMTO-ASR and its advantages have been extensively discussed earlier in a review by Mookerjee [3] and in a series of articles [5,28–32]. We would like to refer the interested readers to these for details.

## **2. Spectral functions, complex bands and density of states for 50-50 CuZn**

In this section we shall introduce the salient features of the ASR which will be required by us in our subsequent discussions.

We shall start from a first principle TB-LMTO set of orbitals [33,34] in the most-localized representation. This is necessary, because the subsequent recursion requires a sparse representation of the Hamiltonian. The TB-LMTO second-order tight-binding Hamiltonian  $\mathbf{H}^{(2)}$  is described by a set of potential parameters:  $\mathbf{C}_R$ ,  $\mathbf{E}_{\nu R}$ ,  $\mathbf{\Delta}_R$  and  $\mathbf{o}_R$  which are the characteristics of the atoms which sit on the lattice sites labelled by  $R$ , and a structure matrix  $\mathbf{S}_{RR'}$  which is characteristic of the lattice on which the atoms sit. For a substitutionally disordered alloy, the structure matrix is not random but the potential parameters are and can be described by a set of random occupation variables  $\{n_R\}$ . We may write

$$C_{RL} = C_L^A n_R + C_L^B (1 - n_R)$$

and similar expressions for the other potential parameters. The random site-occupation variables  $\{n_R\}$  take values 1 and 0 depending upon whether the muffin-tin labelled by  $R$  is occupied by A or B-type of atom. The atom sitting at  $\{R\}$  can either be of type A ( $n_R = 1$ ) with probability  $x$  or B ( $n_R = 0$ ) with probability  $y$ .

In the absence of short-range order, the augmented space formalism associates with each random variable  $n_R$  an operator  $\mathbf{M}_R$  whose spectral density is its probability density.

$$p(n_R) = -\frac{1}{\pi} \lim_{\delta \rightarrow 0} \text{Im} \langle \uparrow_R | ((n_R + i\delta)\mathbf{I} - \mathbf{M}_R)^{-1} | \uparrow_R \rangle.$$

The operator  $\mathbf{M}_R$  acts on the ‘configuration space’ of the variable  $n_R$ ,  $\Phi_R$  spanned by the configuration states  $|\uparrow_R\rangle$  and  $|\downarrow_R\rangle$ . The augmented space theorem [28] states that a configuration average can be expressed as a matrix element in the ‘configuration space’ of the disordered system:

$$\langle \langle A(\{n_R\}) \rangle \rangle = \langle \{\emptyset\} | \tilde{\mathbf{A}}(\{\mathbf{M}_R\}) | \{\emptyset\} \rangle, \quad (1)$$

where

$$\tilde{\mathbf{A}}(\{\tilde{\mathbf{M}}_R\}) = \int \dots \int A(\{\lambda_R\}) \prod d\mathbf{P}(\lambda_R).$$

$\mathbf{P}(\lambda_R)$  is the spectral density of the self-adjoint operator  $\tilde{\mathbf{M}}_R$ , and the configuration state  $|\{\emptyset\}\rangle$  is  $\prod_R^\otimes |\uparrow_R\rangle$ . Applying (1) to the Green function we get

$$\langle \langle \mathbf{G}(\mathbf{k}, z) \rangle \rangle = \langle \mathbf{k} \otimes \{\emptyset\} | (z\tilde{\mathbf{I}} - \tilde{\mathbf{H}}^{(2)})^{-1} | \mathbf{k} \otimes \{\emptyset\} \rangle, \quad (2)$$

where  $\mathbf{G}$  and  $\mathbf{H}^{(2)}$  are operators which are matrices in angular momentum space, and the augmented  $\mathbf{k}$ -space basis  $|\mathbf{k}, L \otimes \{\emptyset\}\rangle$  has the form

$$(1/\sqrt{N}) \sum_R \exp(-i\mathbf{k} \cdot R) |R, L \otimes \{\emptyset\}\rangle.$$

The augmented space Hamiltonian  $\tilde{\mathbf{H}}^{(2)}$  is constructed from the TB-LMTO Hamiltonian  $\mathbf{H}^{(2)}$  by replacing each random variable  $n_R$  by the operators  $\tilde{\mathbf{M}}_R$ . It is an operator in the augmented space  $\Psi = \mathcal{H} \otimes \prod_R^\otimes \Phi_R$ . The ASF maps a disordered Hamiltonian described in a Hilbert space  $\mathcal{H}$  onto an ordered Hamiltonian in an enlarged space  $\Psi$ , where the space  $\Psi$  is constructed as the outer product of the space  $\mathcal{H}$  and configuration space  $\Phi$  of the random variables of the disordered Hamiltonian. The configuration space  $\Phi$  is of rank  $2^N$  if there are  $N$  muffin-tin spheres in the system. Another way of looking at  $\tilde{\mathbf{H}}^{(2)}$  is to note that it is the collection of all possible Hamiltonians for all possible configurations of the system.

This equation is now exactly in the form in which recursion method may be applied. At this point we note that the above expression for the averaged  $G_{LL}(\mathbf{k}, z)$  is exact.

The recursion method addresses inversions of infinite matrices of the type associated with the Green function [35]. Once a sparse representation of an operator in Hilbert space,  $\tilde{\mathbf{H}}^{(2)}$ , is known in a countable basis, the recursion method obtains an alternative basis in which the operator becomes tridiagonal. This basis and the

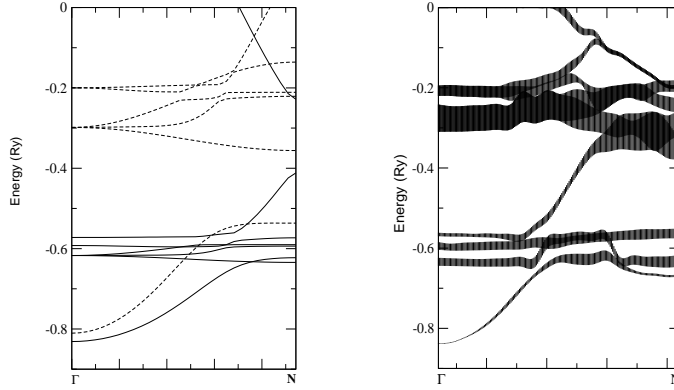


**Figure 1.** (left) Bands for pure Cu and Zn in bcc lattices with the same lattice parameter as the 50-50 CuZn alloy. The dashed lines are for Cu and the full lines for Zn. (right) Complex bands for the 50-50 CuZn alloy.

representations of the operator in it are found recursively through a three-term recurrence relation. The spectral function is then obtained from the continued fraction:

$$\begin{aligned}
 \langle\langle G_{LL}(\mathbf{k}, z) \rangle\rangle &= \frac{\beta_{1L}^2}{z - \alpha_{1L}(\mathbf{k}) - \frac{\beta_{2L}^2(\mathbf{k})}{z - \alpha_{2L}(\mathbf{k}) - \frac{\beta_{3L}^2(\mathbf{k})}{\ddots}}} \\
 &= \frac{\beta_{1L}^2}{z - E_L(\mathbf{k}) - \Sigma_L(\mathbf{k}, z)}, \tag{3}
 \end{aligned}$$

where  $\Gamma_L(\mathbf{k}, z)$  is the asymptotic part of the continued fraction. The approximation involved has to do with the termination of this continued fraction. The coefficients are calculated exactly up to a finite number of steps  $\{\alpha_n, \beta_n\}$  for  $n < N$  and the asymptotic part of the continued fraction is obtained from the initial set of coefficients using the idea of Beer and Pettifor terminator [36]. Haydock and coworkers [37] have carried out extensive studies of the errors involved and precise estimates are available in the literature. Haydock [38] has shown that if we carry out recursion exactly up to  $N$  steps, the resulting continued fraction maintains the first  $2N$  moments of the exact result.

The self-energy  $\Sigma_L(\mathbf{k}, z)$  arises because of scattering by the random potential fluctuations.

The average spectral function  $\langle\langle A_{\mathbf{k}}(E) \rangle\rangle$  is related to the averaged Green function in reciprocal space as

$$\langle\langle A_{\mathbf{k}}(E) \rangle\rangle = \sum_L \langle\langle A_{\mathbf{k}L}(E) \rangle\rangle,$$

where

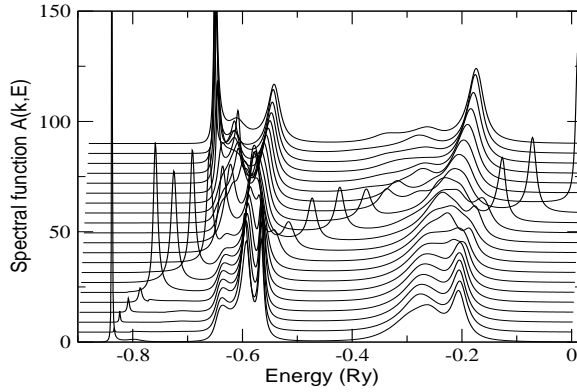


**Figure 2.** Spectral functions for the CuZn alloy for  $\mathbf{k}$ -vectors along the  $\Gamma$  to  $N$  direction in the Brillouin zone.

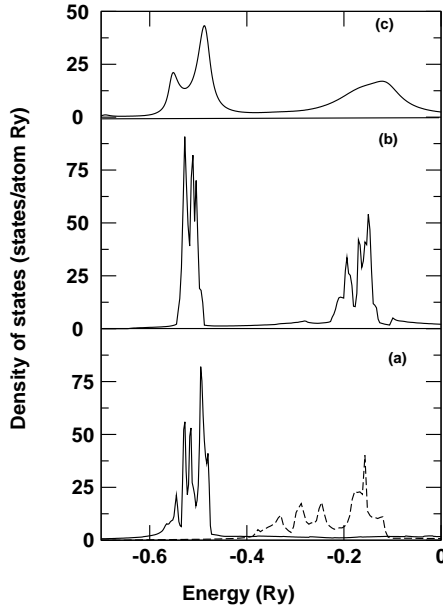


**Figure 3.** (a) Density of states of pure Zn (solid line) and Cu (dashed line) in the same bcc lattice as the 50-50 CuZn alloy. (b) Density of states for ordered B2 50-50 CuZn alloy. (c) Density of states for the disordered bcc 50-50 CuZn alloy. These results are comparable to the single-site CPA.

$$\langle\langle A_{\mathbf{k}L}(E) \rangle\rangle = -\frac{1}{\pi} \lim_{\delta \rightarrow 0^+} \{\text{Im} \langle\langle G_{LL}(\mathbf{k}, E - i\delta) \rangle\rangle\}.$$

To obtain the complex bands for the alloy we fix a value for  $\mathbf{k}$  and solve for

$$z - E_L(\mathbf{k}) - \Sigma_L(\mathbf{k}, E) = 0.$$

The real part of the roots will give the position of the bands, while the imaginary part of roots will be proportional to the disorder-induced broadening. Since the alloy is random, the bands always have finite lifetimes and are fuzzy.

We have used this reciprocal space ASR to obtain the complex bands and spectral functions for the CuZn alloy. This is shown in figures 1 and 2. It should be noted that we have carried out a fully LDA self-consistent calculation using the TB-LMTO-ASR developed by us [39] to obtain the potential parameters. It takes care of the charge transfer effects. For the Madelung energy part of the alloy calculation, we have chosen the approach of Ruban and Skriver [40].

The two panels of figure 1 compare the band structures of pure Cu and pure Zn metals in the same bcc lattice as the 50-50 alloy. We note that the *s*-like bands of Cu and Zn stretch from  $-0.8$  Ry, while the *d*-like states of Zn and Cu, whose degeneracies are lifted by the cubic symmetry of the bcc lattice are more localized and reside in the neighbourhood of  $-0.6$  Ry and between  $-0.3$  and  $-0.2$  Ry respectively. The complex bands of the solid clearly reflect the same band structure. However, the bands are slightly shifted and broadened because of the disorder scattering of Bloch states in the disordered alloy. The broadening due to disorder scattering is maximum for the Cu *d*-like bands, less for the Zn *d*-like bands and minimum for the lower *s*-like bands. This is because Cu and Zn atoms do not present much fluctuation in the potential for the *s*-like states.

The same is reflected in the spectral functions, shown here also along the  $\Gamma$ - $N$  direction in the Brillouin zone. We see sharp peaks stretching from  $-0.8$  Ry, groups of wider peaks around  $-0.6$  Ry with less dispersion, characteristic of the more localized *d*-like states and groups of much wider peaks straddling  $-0.3$ - $0.2$  Ry also with less dispersion. The spectral functions play an important role in response functions related to photoemission and optical conductivity [41]. Our complex bands agree remarkably well with figure 3 of Bansil and Ehrenreich [10]. These authors of course did not show the dispersion of the Zn *d*-bands, but as in their work, the Cu bands show greater disorder-induced broadening than the lower energy Zn *d*-bands.

We may use the generalized tetrahedron method to pass from the reciprocal space spectral functions to the real space density of states [42]. Alternatively, we may also carry out real-space ASR to obtain the density of states directly.

Figure 3 shows the densities of states for the pure Zn (solid lines) and Cu (dashed lines) in the same bcc lattice as the alloy and compares this with the ordered B2 and disordered bcc 50-50 CuZn alloy. We first note that in the ordered B2 alloy there is a considerable narrowing of the Zn well as the Cu *d*-like bands. The feature around  $-0.35$  Ry below the Fermi energy is suppressed in the ordered alloy. In the disordered alloy on the other hand, although disorder scattering introduces life-time effects which washes out the sharp structures in the ordered systems, the resemblance to the pure metals is evident. As seen in the complex bands, the life-time effects in the Cu *d*-like part is prominent. If we interpret figure 3a as due to completely segregated Cu-Zn and figure 3b as the completely ordered one, then the disordered alloy lies between the two. In the next section, introducing short-range ordering effects on top of the fully disordered alloy, we shall study how to bridge between the two states.

### 3. Short-ranged ordering in the alloys

Attempts at developing generalizations of the coherent potential approximation (CPA) to include effects of short-range order (SRO) have been many, spread over the last several decades. The CPA being a single site mean-field approximation could not take into account SRO, since any description of SRO had to take into account correlations in, at least, a nearest-neighbour cluster on the lattice. The early attempts to generalize the CPA to clusters were beset with difficulties of violation of the analytic properties of the approximated configuration averaged Green function. Tsukada's [43] idea of introducing a super-cell of the size of the cluster immersed in an effective medium suffered from the problem of broken translational symmetry within the cluster even when the disorder was homogeneous. The CCPA proposed by Kumar *et al* [44] based on the augmented space theorem also suffered from the same problem. The embedded cluster approximation of Gonis *et al* [45] immersed a cluster in a CPA medium which lacked the full self-consistency with it. The first translationally symmetric cluster approximations which preserved the analytic properties of the approximate Green functions were all based on the augmented space theorem of Mookerjee [28]. They included the travelling cluster approximation (TCA) of Kaplan and Gray [29] and Mills and Ratanavararaksa [46] and the CCPA proposed by Razee *et al* [47]. The problem with these approaches was that they became intractable as the size of the cluster was increased much beyond two sites. Mookerjee and Prasad [48] generalized the augmented space theorem to include correlated disorder. However, since they then went on to apply it in the CCPA approximation, they could not go beyond the two-site cluster and they applied the method to model systems alone. The breakthrough came with the augmented space recursion (ASR) proposed by Saha *et al* [49,50]. The method was a departure from the mean-field approaches which always began by embedding a cluster in an effective medium which was then obtained self-consistently. Here the Green function was expanded in a continued fraction whose asymptotic part was approximately estimated from its initial steps through an ingenious termination procedure [35]. In this method the effect at a site of quite a large environment around it could be taken into account depending how far one went down the continued fraction before termination. The technique was made fully LDA-self-consistent within TB-LMTO approach [51] and several applications have been carried out to include short-range order in different alloy systems [52]. Recently, Leath and co-workers have developed an itinerant CPA (ICPA) based on the augmented space theorem [53], which also maintains both analyticity and translational symmetry and takes into account effect of the nearest neighbour environment of a site in an alloy. The technique has been successfully applied to the phonon problem in alloys where there were large force constant disorders. The results of this method for NiPd and NiPt alloys match well with the ASR applied to the same alloys [54] and there is now an effort to apply the ICPA to electronic problems based on both the TB-KKR and the TB-LMTO methods. A very different and rather striking approach has been developed by Rowlands *et al* [55] (the non-local CPA or NL-CPA) using the idea of coarse graining in reciprocal space originally proposed by Jarrell and Krishnamurthy [12]. The NL-CPA with SRO has been applied earlier by Rowlands *et al* [11] and is on the verge of being made fully DFT self-consistent within the KKR. The authors

report an unpublished report on it [56]. In this communication we report a fully DFT self-consistent ASR based on the TB-LMTO with SRO incorporated. We have applied it to the case of 50-50 CuZn alloys, so as to have a comparison with earlier attempts using different techniques.

#### 4. The generalized augmented space theorem

The generalized augmented space theorem has been described in detail by Mookerjee and Prasad [48]. Let us briefly introduce those essential ideas which are necessary to make this communication reasonably self-contained.

For a substitutionally binary disordered alloy  $A_xB_y$  on a lattice we can introduce a set of random occupation variables  $\{n_R\}$  associated with the lattice sites labelled by  $R$ , which take the values 0 or 1 depending upon whether the site  $R$  is occupied by a A- or a B-type of atom. The Hamiltonian and hence the Green function are both functions of this set of random variables.

To start with, let us assume that short-range order extends up to nearest neighbours only. Let us take as an example the nearest-neighbour cluster of nine atoms on a body centered cubic lattice centered on the site labelled  $R_0$ . The occupation variables associated with its eight neighbours are correlated with  $n_{R_0}$ , but not with one another. Further, none of the other occupation variables associated with more distant sites are correlated with  $n_{R_0}$ .

We may then write

$$P(n_{R_0}, n_{R_1}, \dots, n_{R_k} \dots) = P(n_{R_0}) \prod_{j=1}^8 P(n_{R_j} | n_{R_0}) \prod_{k>8} P(n_{R_k}).$$

The generalized augmented space theorem then associates with the random variables  $\{n_{R_k}\}$  corresponding operators  $\{M_{R_k}\}$  in their configuration space. The construction of the representations of these operators has been discussed in detail in the paper by Mookerjee and Prasad [48]. Here we shall quote only the relevant results necessary to proceed further.

We shall characterize the SRO by a Warren-Cowley parameter  $\alpha$ . In terms of this the probability densities are given by

For  $k = 0$  and  $k > 8$

$$P(n_{R_k}) = x\delta(n_{R_k} - 1) + y\delta(n_{R_k}), \quad x + y = 1.$$

For  $1 \leq j \leq 8$

$$\begin{aligned} P(n_{R_j} | n_{R_0} = 1) &= (x + \alpha y)\delta(n_{R_j} - 1) + (1 - \alpha)y\delta(n_{R_j}), \\ P(n_{R_j} | n_{R_0} = 0) &= (1 - \alpha)x\delta(n_{R_j} - 1) + (y + \alpha x)\delta(n_{R_j}). \end{aligned}$$

In the full augmented space, the operators which replace the occupation variables are

$$\begin{aligned} \widetilde{M}_{R_0} &= M_{R_0} \otimes I \otimes I \otimes \dots, \\ \widetilde{M}_{R_j} &= \sum_{\lambda=0}^1 P_1^\lambda \otimes M_{R_j}^\lambda \otimes I \otimes \dots, \quad j = 1, 2, \dots, 8 \end{aligned}$$

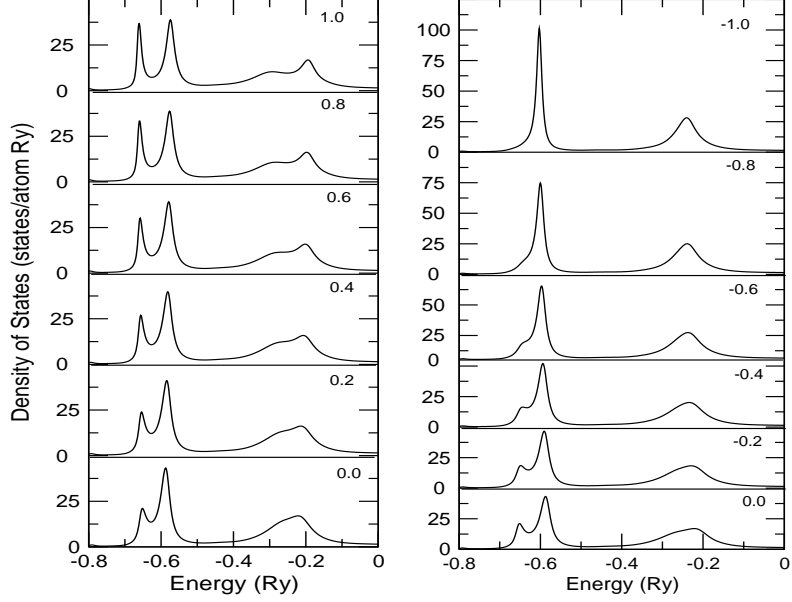


**Figure 4.** Density of states for 50-50 CuZn with (left) increasing positive  $\alpha$  which indicates increasing clustering tendency and (right) increasing negative  $\alpha$  which indicates ordering tendency. The values of the SRO parameter  $\alpha$  are shown on the upper right corner of each panel. Energies are shown with respect to the Fermi energy placed at the origin.

$$\widetilde{\mathbf{M}}_k = I \otimes I \otimes \dots M_{R_k} \otimes I \otimes \dots, \quad k > 8$$

$$P(n_{R_j} | n_{R_0} = \lambda) = -\frac{1}{\pi} \lim_{\delta \rightarrow 0} \text{Im} \langle \uparrow_{R_j} | ((n_{R_j} + i\delta) - M_{R_j}^\lambda)^{-1} | \uparrow_{R_j} \rangle. \quad (4)$$

We now follow the augmented space theorem and replace all the occupation variables  $\{n_R\}$  by their corresponding operators. The configuration average is the specific matrix element between the reference state  $|\{\emptyset\}\rangle$  as discussed earlier. We also note that the choice of the central site labelled  $R_0$  is immaterial. If we translate this site to any other and apply the lattice translation to all the sites, the Hamiltonian in the full augmented space remains unchanged. This formulation of short-ranged order also possesses lattice translational symmetry, provided the short-range order is homogeneous in space.

## 5. Effect of SRO on the density of states

We have carried out the TB-LMTO-ASR calculations on CuZn with a lattice constant of 2.85 Å. The Cu and Zn potentials are obtained from the LDA self-consistency loop. All reciprocal space integrals are carried out using the generalized tetrahedron integration for disordered systems introduced by us earlier [42].

Let us discuss the effect of SRO, leading, on one hand to ordering ( $\alpha < 0$ ) and on the other and to segregation ( $\alpha > 0$ ). We shall first look at figures 1 and 3. The complex band structure shown in figure 1 shows that the system is a split band alloy. The positions of the  $d$ -bands of Cu and Zn are well-separated in energy. This implies that the ‘electrons travel more easily between Cu or between Zn sites than between unlike ones’ [11]. So when the alloy orders and unlike sites sit next to each other, the overlap integral between the like sites decreases. This leads to a narrowing of the bands associated with Cu and Zn. A comparison between the bottom and central panels of figure 3 shows that the bands in the latter are much narrower than those of the former. This is the main effect of ordering setting in. On the other hand, when the alloy is completely disordered, the bands gets widened by disorder scattering and the sharp structures in the density of states are smoothened.

Figure 4 (left panel) shows the density of states with increasing positive  $\alpha$  indicating increasing clustering tendency. Comparing with figure 3 we note that as clustering tendency increases the density of states begins to show the structures seen in the pure metals in both the split bands. For large positive  $\alpha$  there is still residual long-ranged disorder. This causes smoothening of the bands with respect to the pure materials. For these large, positive  $\alpha$ s, we notice the development of the structure around  $-0.35$  Ry below the Fermi energy.

Figure 4 (right panel) shows the density of states with increasing negative  $\alpha$  indicating increasing ordering tendency. On the bcc lattice at 50-50 composition we expect this ordering to favour a B2 structure. With increasing ordering tendency, both the split bands narrow and lose structure. The feature around  $-0.35$  Ry disappears. This band narrowing and suppression of the feature around  $-0.35$  Ry are clearly seen in the ordered B2 alloy shown in figure 3b.

Our analysis is closely similar to that of Rowlands *et al* [11]. Although there are differences in the way short-range order is introduced in the ASR and NL-CPA, there is broad agreement between the two works on the effect of short-range ordering. In particular, the development of the shoulder around  $-0.35$  Ry below the Fermi energy with segregation and the narrowing of the split bands on ordering are observed in both the approaches. In the ordering regime there are minor differences in the results of the two approaches. The relative heights of the two peaks in the split bands are much more pronounced and the broadening is larger in the ASR when compared with NL-CPA.

Finally, in figure 5 we show the band energy as a function of the nearest-neighbour Warren-Cowley parameter. The minimum occurs at the ordering end, as expected. Experimentally the alloy does show a tendency to order at lower temperatures.

## 6. Concluding remarks

The work presented here is a part of our continuing development of methods for the study of electronic structure of disordered alloys based on the augmented space method introduced by one of us. We have argued that our generalization of the augmented space technique to include correlated disorder and its combination with the recursion method of Haydock *et al* [35], yields configuration averaged Green functions which are lattice translationally symmetric and have the necessary herglotz analytical properties of the exact ones. We have applied this technique to

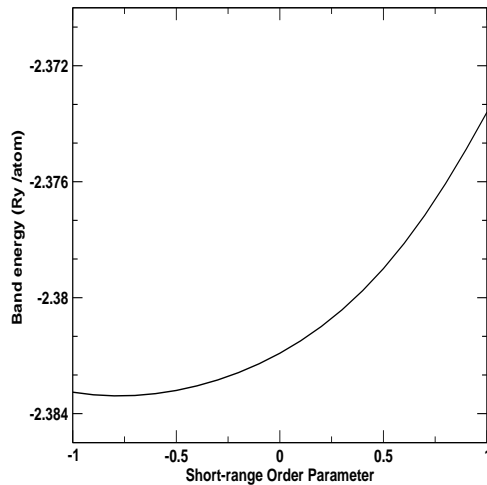


**Figure 5.** The band energy (from which the contribution of the core electrons have been subtracted) as a function of the nearest-neighbour Warren-Cowley SRO parameter.

the case of the split-band 50-50 CuZn alloy. Experimental evidences of short-range ordering in this alloy exist and hence our interest in its study. We have looked at the whole range of short-range ordering from clustering to homogeneous disorder to ordering and have studied its effect on the density of states, optical conductivity and reflectivity of the alloy. Our results are in broad agreement with an alternative approach via the non-local-CPA.

We had set out to demonstrate that the generalized augmented space recursion, in combination with the LDA-based TB-LMTO, is an efficient computational technique which can go beyond the single-site mean-field approximation and take into account local environmental effects like short-range ordering and clustering, at the same time maintaining analytic properties essential for physical interpretation of its results. This is the main conclusion of this work.

### Acknowledgment

One of us (KT) would like to acknowledge the CSIR for financial assistance.

### References

- [1] P E A Turchi, L Reihard and G M Stocks, *Phys. Rev.* **B50**, 15542 (1994)
- [2] A Zunger, S-H Wei, L G Ferreira and J Bernard, *Phys. Rev. Lett.* **65**, 353 (1990)
- [3] A Mookerjee, in *Electronic structure of alloys, surfaces and clusters* edited by D D Sarma and A Mookerjee (Taylor-Francis, UK, 2003)
- [4] S Ghosh, P L Leath and M H Cohen, *Phys. Rev.* **B66**, 214206 (2002)
- [5] T Saha, I Dasgupta and A Mookerjee, *J. Phys.: Condens. Matter* **6**, L245 (1994)
- [6] A Chakrabarti and A Mookerjee, *Europhys. J.* **B44**, 21 (2005)

- [7] F Jona and P M Marcus, *J. Phys.: Condens. Matter* **13**, 5507 (2001)
- [8] *Binary alloy phase diagrams* edited by T B Massalski, H Okamoto, P R Subramaniam and L Kacprzak (ASM International, Materials Park, Ohio, 1990)
- [9] W Hume-Rothery, *The structure of metals and alloys* (Institute of Metals, London, 1936)
- [10] A Bansil and H Ehrenreich, *Phys. Rev.* **B9**, 445 (1974)
- [11] D A Rowlands, J B Staunton, B L Gyorffy, E Bruno and B Ginatempo, *Phys. Rev.* **B72**, 045101 (2005)
- [12] M Jarrell and H R Krishnamurthy, *Phys. Rev.* **B63**, 125102 (2001)
- [13] C B Walker and D T Keating, *Phys. Rev.* **130**, 1726 (1963)
- [14] C B Walker and D R Chipman, *Phys. Rev.* **B4**, 3104 (1971)
- [15] I A Abrikosov, A M N Niklasson, S I Simak, B Johansson, A V Ruban and H L Skriver, *Phys. Rev. Lett.* **76**, 4203 (1996)
- [16] I A Abrikosov, Yu H Velikov, P A Korzhavyi, A V Ruban and L E Shilkrot, *Solid State Commun.* **83**, 867 (1992)
- [17] D D Johnson and F J Pinski, *Phys. Rev.* **B48**, 11553 (1993)
- [18] P P Singh, A Gonis and P E A Turchi, *Phys. Rev. Lett.* **71**, 1605 (1993)
- [19] P P Singh and A Gonis, *Phys. Rev.* **B49**, 1642 (1994)
- [20] P A Korzhavyi, A V Ruban, I A Abrikosov and H L Skriver, *Phys. Rev.* **B51**, 5773 (1995)
- [21] Y Wang, G M Stocks, W A Shelton, D M C Nicholson, Z Szotek and W M Temmerman, *Phys. Rev. Lett.* **75**, 2867 (1995)
- [22] E Bruno, L Zingales and A Milici, *Phys. Rev.* **B66**, 245107 (2002)
- [23] L Muldower, *Phys. Rev.* **127**, 1551 (1963)
- [24] G Joos and A Klopfer, *Z. Physik.* **138**, 251 (1954)
- [25] H Amar and K H Johnson, *Phys. Rev.* **139**, A760 (1965)
- [26] H Amar, K H Johnson and K P Wang, *Phys. Rev.* **148**, 672 (1966)
- [27] H Amar, K H Johnson and C B Sommers, *Phys. Rev.* **153**, 655 (1967)
- [28] A Mookerjee, *J. Phys.* **C6**, 1340 (1973)
- [29] T Kaplan and L J Gray, *Phys. Rev.* **15**, 3260 (1977)
- [30] T Saha, I Dasgupta and A Mookerjee, *J. Phys.: Condens. Matter* **8**, 1979 (1996)
- [31] S Ghosh, N Das and A Mookerjee, *Int. J. Mod. Phys.* **B21**, 723 (1999)
- [32] I Dasgupta, T Saha, A Mookerjee and G P Das, *J. Phys.: Condens. Matter* **9**, 3529 (1997)
- [33] O K Andersen, *Phys. Rev.* **12**, 3060 (1975)
- [34] O K Andersen and O Jepsen, *Phys. Rev. Lett.* **53**, 2571 (1984)
- [35] R Haydock, *Solid state physics* (Academic Press, New York, 1980) vol. 35
- [36] N Beer and D G Pettifor, in *The electronic structure of complex systems* edited by P Phariseau and W M Temmerman (Plenum, New York, 1982) vol. 113, p. 769
- [37] R Haydock, *Philos. Mag.* **B43**, 203 (1981)  
R Haydock and R L Te, *Phys. Rev.* **49**, 10845 (1994)
- [38] R Haydock, *Real space techniques in electronic structure*, Thesis (University of Cambridge, UK, 1972)
- [39] A Chakrabarty and A Mookerjee, *Euro. Phys. J.* **B44**, 21 (2005)
- [40] A V Ruban and H L Skriver, *Phys. Rev.* **B66**, 024201 (2003)
- [41] K K Saha and A Mookerjee, *J. Phys.: Condens. Matter* **17**, 4559 (2005)
- [42] K K Saha, A Mookerjee and O Jepsen, *Phys. Rev.* **B71**, 094207 (2005)
- [43] M Tsukada, *J. Phys. Soc. Jpn.* **32**, 1475 (1972)
- [44] V Kumar, V K Srivastava and A Mookerjee, *J. Phys.* **C15**, 1939 (1982)
- [45] A Gonis, G M Stocks, W H Butler and H Winter, *Phys. Rev.* **B29**, 555 (1984)

*Electronic structure of binary alloys*

- [46] R Mills and P Ratanavararaksa, *Phys. Rev.* **B18**, 5291 (1978)
- [47] S S A Razee, S S Rajput, R Prasad and A Mookerjee, *Phys. Rev.* **B42**, 9391 (1990)
- [48] A Mookerjee and R Prasad, *Phys. Rev.* **B48**, 17724 (1993)
- [49] T Saha, I Dasgupta and A Mookerjee, *Phys. Rev.* **B50**, 13267 (1994)
- [50] T Saha, I Dasgupta and A Mookerjee, *J. Phys.: Condens. Matter* **8**, 1979 (1996)
- [51] A Chakrabarti and A Mookerjee, *Euro. Phys. J.* **B44**, 21 (2005)
- [52] D Paudyal, T Saha-Dasgupta and A Mookerjee, *J. Phys.: Condens. Matter* **16**, 2317 (2004)
- [53] S Ghosh, P L Leath and M H Cohen, *Phys. Rev.* **B66**, 214206 (2002)
- [54] A Alam and A Mookerjee, *Phys. Rev.* **B69**, 024205 (2004)
- [55] D A Rowlands, J B Staunton and B L Györfy, *Phys. Rev.* **B67**, 115109 (2003)
- [56] D A Rowlands, J B Staunton, B L Györfy, E Bruno and B Ginatempo, cond-mat/0411347